ELSEVIER

January 2003

Materials Letters 57 (2003) 1096–1102

MATERIALS LETTERS

www.elsevier.com/locate/matlet

Some factors influencing forced hydrolysis of $FeCl_3$ solutions

S. Musić [a,*], S. Krehula [a], S. Popović [b], Ž. Skoko [b]

[a] *Division of Materials Chemistry, Rudjer Bošković Institute, P.O. Box 180, HR-10002 Zagreb, Croatia*
[b] *Department of Physics, Faculty of Science, University of Zagreb, P.O. Box 331, HR-10002 Zagreb, Croatia*

Received 30 May 2002; accepted 31 May 2002

Abstract

Phase composition, size and shape of iron oxide particles produced by forced hydrolysis of Fe^{3+} ions depended on the concentrations of $FeCl_3$ and HCl, and on the presence of 0.005 M quinine hydrogen sulphate (QHS). After 7 days of forced hydrolysis, α-Fe_2O_3 was produced from the 0.01 M $FeCl_3$ solution, the mixture of β-FeOOH and α-Fe_2O_3 was produced from 0.02 M $FeCl_3$ solution, whereas β-FeOOH was produced from the 0.1 M $FeCl_3$ solution. Forced hydrolysis of the 0.1 M $FeCl_3$ + 0.1 M HCl solution yielded α-Fe_2O_3. In the presence of 0.005 M QHS, the formation of β-FeOOH and α-Fe_2O_3 was partially or completely suppressed in dependence on the conditions of forced hydrolysis of Fe^{3+} ions. Specific shapes of β-FeOOH particles (cigar-type, X-, Y-, and star-shapes) were not obtained in the presence of 0.005 M QHS. The bundles of β-FeOOH needles with irregular ends were obtained instead. Also, in the presence of 0.005 M QHS, the formation of α-FeOOH is favoured. The preferential adsorption of sulphate groups and a possible influence of quinine group at the very beginning of $FeCl_3$ hydrolysis were suggested as responsible for the effects observed.

Keywords: $FeCl_3$ hydrolysis; α-FeOOH; β-FeOOH; α-Fe_2O_3; Quinine hydrogen sulphate

1. Introduction

In several past decades, the phenomena related to slow and forced hydrolysis of Fe^{3+} ions in aqueous media were extensively investigated from the academic point of view [1,2]. These phenomena play a significant role in the transport of iron in natural aquatic systems, as well as in the iron cycle in living organisms [3]. Iron(III)-oxyhydroxides and -oxides are the solid products of hydrolysis of Fe^{3+} ions, and they are often cited in the reference literature under a general name, *iron oxides*. Synthetic iron oxides have found various applications as pigments, catalysts, magnetic materials, sensors, etc. Analogies between the precipitation of iron oxides and their phase transformations in aqueous media on one side and the rusting of steel on the other, were observed.

The precipitation of iron oxides by hydrolysis of Fe^{3+} ions in aqueous media depends on the type of Fe(III)-salt and its concentration, pH, the presence of a complexing agent, temperature and time [4–7]. The presence of sodium polyanethol sulphonate in hydrolysing $FeCl_3$ solutions influenced the size and shape of β-FeOOH particles [8]. The influences of various amines [9] and dioxane [10] on the shape of α-Fe_2O_3 particles, produced by forced hydrolysis of $FeCl_3$

* Corresponding author.
E-mail address: music@rudjer.irb.hr (S. Musić).

0167-577X/02/$ - see front matter © 2002 Elsevier Science B.V. All rights reserved.
PII: S0167-577X(02)00937-0

Table 1
Experimental conditions of the Fe^{3+} hydrolysis in aqueous solutions at 90 °C and the phase composition of samples as determined by XRD

Sample	$[FeCl_3]$/M	[HCl]/M	[QHS]/M	Time of heating (days)	Phase composition as found by XRD (approximate molar fraction)
S1	0.01			7	α-Fe_2O_3
S2	0.01		0.005	7	α-FeOOH
S3	0.01	0.05	0.005	7	α-FeOOH
S4	0.02			7	β-FeOOH (0.8) + α-Fe_2O_3 (0.2)
S5	0.02		0.005	7	α-FeOOH
S6	0.02	0.05	0.005	7	α-FeOOH
S7	0.1			1	β-FeOOH
S8	0.1		0.005	1	β-FeOOH
S9	0.1			7	β-FeOOH
S10	0.1		0.005	7	β-FeOOH (0.9) + α-FeOOH (0.1)
S11	0.1	0.005		1	β-FeOOH
S12	0.1	0.005	0.005	1	β-FeOOH
S13	0.1	0.005		7	β-FeOOH
S14	0.1	0.005	0.005	7	β-FeOOH (0.9) + α-FeOOH (0.1)
S15	0.1	0.05	0.005	7	α-FeOOH
S16	0.1	0.1		7	α-Fe_2O_3
S17	0.1	0.1	0.005	7	no visible precipitate

solutions, were also observed. The presence of metal ions (Cu^{2+} or Cr^{3+}) in hydrolysing $FeCl_3$ solutions inhibited the growth of β-FeOOH particles at lower concentrations, whereas the growth of β-FeOOH particles was promoted at higher concentrations of these metal ions [11]. Ellipsoidal α-Fe_2O_3 particles were produced by forced hydrolysis of $FeCl_3$ solutions in the presence of a small amount of phosphates [12–15]. Forced hydrolysis of $Fe(ClO_4)_3$ solutions with decomposing urea yielded only α-Fe_2O_3 particles and their shape was also modified by the presence of a small amount of phosphates [16].

In the present work, we have investigated forced hydrolysis of $FeCl_3$ solutions with a focus on the properties of the solid phase formed by this process. The effects of $FeCl_3$ and HCl concentrations on the phase composition, size and morphology of iron oxide particles have been analysed. The strong effect of quinine hydrogen sulphate (QHS) on the properties of solid hydrolytic products has also been observed. Quinine and its salts have applications in medicine and food technology. It is generally assumed that quinine and its derivatives act in living organisms via the formation of quinine complexes with metal ions. Specifically, the antimalarial action of quinine was explained by its coordination with the iron of heme in erythrocytes of blood infected with the malaria parasites.

2. Experimental

$FeCl_3 \cdot 6H_2O$ and HCl of analytical purity supplied by Kemika were used. Quinine hydrogen sulphate ($C_{20}H_{24}O_2N_2 \cdot H_2SO_4 \cdot 7H_2O$) supplied by BDH was used. All solutions were prepared with doubly distilled water. Experimental conditions for the preparation of the precipitation systems are given in Table 1. Aging of the precipitation systems was performed in glass autoclaves at 90 °C. After a proper aging time, solid hydrolytic products were separated from the mother liquor using an ultraspeed centrifuge (Sorvall RC2-B, operational range up to 20,000 rpm). The solid hydrolytic products were subsequently washed with doubly distilled water, and then dried. All solid hydrolytic products were characterized by X-ray powder diffraction (XRD), Fourier transform infrared (FT-IR) spectroscopy and transmission electron microscopy (TEM).

3. Results and discussion

Figs. 1 and 2 show characteristic XRD patterns of selected samples, whereas the phase compositions of all samples are given in Table 1. The table shows a strong dependence of the phase composition of the solid hydrolytic products on the experimental con-

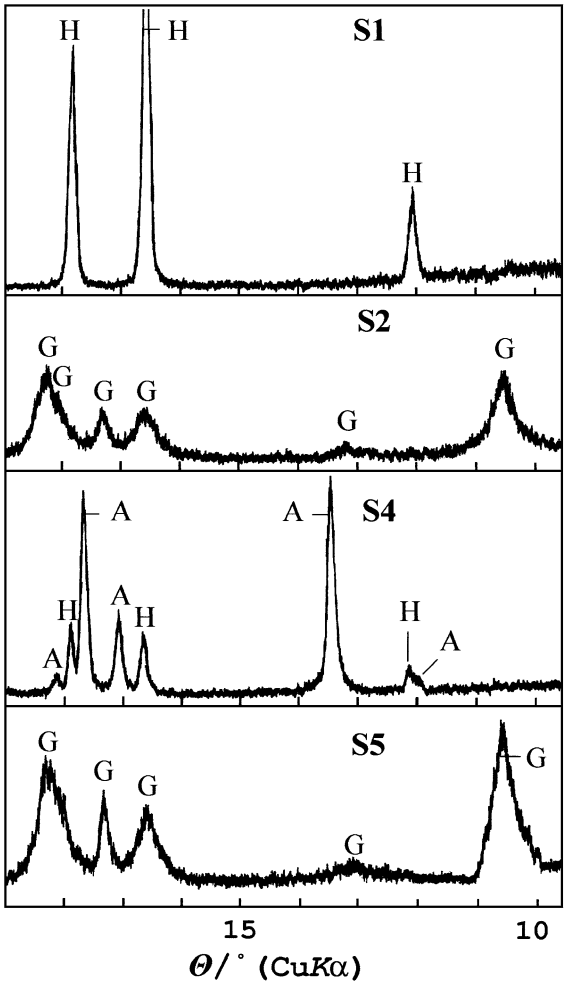

Fig. 1. Characteristic parts of XRD patterns of samples S1, S2, S4 and S5. XRD patterns were measured at room temperature. A=akaganéite; G=goethite; H= hematite.

ditions. After 7 days of forced hydrolysis of the 0.01 M $FeCl_3$ solution α-Fe_2O_3 particles were precipitated, the mixture of β-FeOOH and α-Fe_2O_3 particles was precipitated from the 0.02 M $FeCl_3$ solution, whereas β-FeOOH particles were precipitated from the 0.1 M $FeCl_3$ solution. In the presence of 0.005 M QHS, the formation of β-FeOOH and α-Fe_2O_3 was partially or completely suppressed in dependence on the conditions of forced hydrolysis of Fe^{3+} ions. Forced hydrolysis of the 0.1 M $FeCl_3$ + 0.1 M HCl solution yielded α-Fe_2O_3 after 7 days, whereas the addition of 0.005 M QHS to this precipitation system completely suppressed the formation of a solid hydrolytic product for the same time of aging.

All samples prepared without the QHS addition exhibited sharp diffraction lines, indicating crystallite sizes of the orders of several tens of nanometers. QHS suppressed the growth of crystallites. The samples prepared with an addition of QHS showed a much lower crystallinity (crystallite sizes of several nanometers) than those prepared without QHS. α-FeOOH showed different broadening of diffraction lines corresponding to sets of crystal planes with different indices, indicating an anisotropic shape of crystallites elongated in the *c*-direction.

The results of FT-IR phase analysis of the solid hydrolytic products showed a good agreement with those obtained by XRD. The FT-IR spectra of selected samples are shown in Fig. 3. The FT-IR spectrum of sample S1 corresponds to α-Fe_2O_3 as a single phase. Iglesias and Serna [17] reported a dependence of the IR bands on the shape of α-Fe_2O_3 particles. α-Fe_2O_3 spheres showed IR bands at 575, 485, 385 and 360 cm^{-1}, whereas α-Fe_2O_3 laths showed IR bands at 650, 525, 440 and 300 cm^{-1}. The FT-IR spectrum of sample S2 can be ascribed to α-FeOOH as a single phase. The IR band at 3401 cm^{-1} can be assigned to

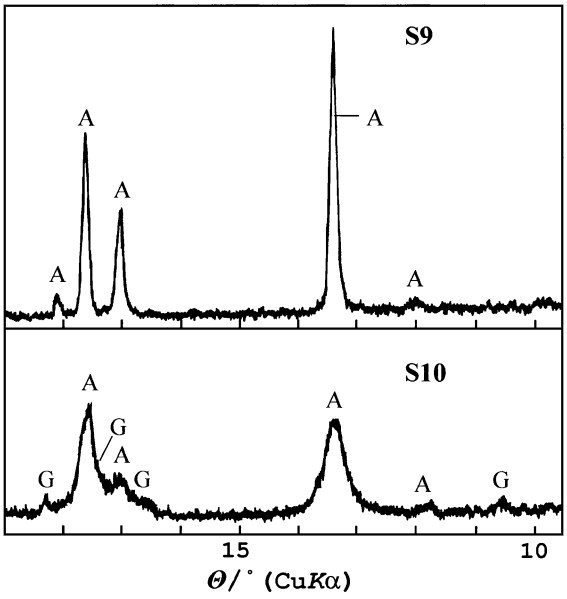

Fig. 2. Characteristic parts of XRD patterns of samples S9 and S10. XRD patterns were measured at room temperature.

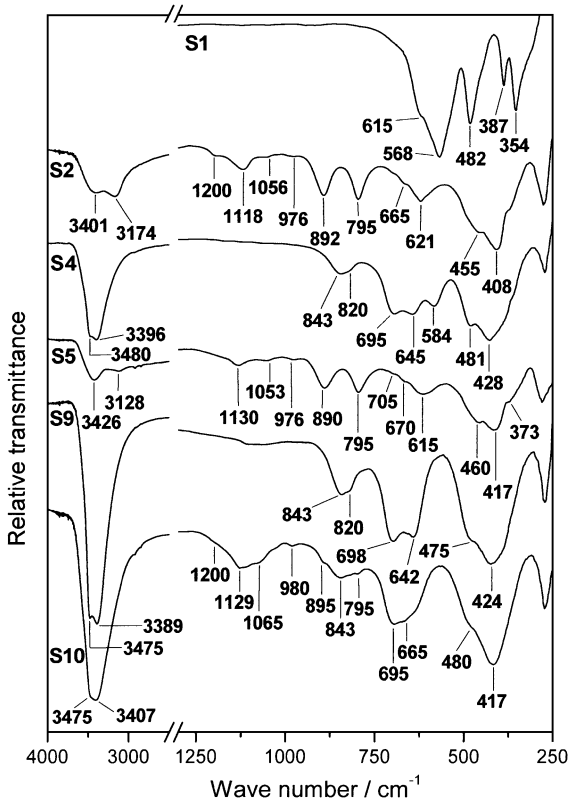

Fig. 3. Fourier transform infrared spectra of selected samples, S1, S2, S4, S5, S9 and S10, recorded at room temperature.

stretching modes of H_2O molecules or to the envelope of hydrogen-bonded surface OH groups, whereas the IR band at 3174 cm^{-1} is due to the presence of the OH stretching mode in α-FeOOH [18]. The bands at 892 and 795 cm^{-1} can be assigned to Fe–O–H bending vibrations in α-FeOOH. In the FT-IR spectrum the bands at 1200, 1118, 1056 and 976 cm^{-1} are also visible and these bands can be ascribed to adsorbed sulphate anions. The origin of these IR bands was reported in a previous work [19].

The FT-IR spectrum of sample S4 indicates the mixture of β-FeOOH and α-Fe_2O_3. α-Fe_2O_3 can be detected in this sample only on the basis of the band at 584 cm^{-1} and partially using the band at 481 cm^{-1}, but this is not sufficient for exact detection of the α-Fe_2O_3 phase. The FT-IR spectrum of sample S9 corresponds to β-FeOOH as a single phase. The FT-IR spectrum of sample S9 shows a doublet at 3475 and 3389 cm^{-1}, a band at 843 cm^{-1} with a shoulder at 820 cm^{-1}, a doublet at 698 and 642 cm^{-1} and a very strong and broad band centred at 424 cm^{-1} with a shoulder at 475 cm^{-1}. In the reference literature there is no full agreement about the nature of OH-stretching bands at 3475 and 3389 cm^{-1}. The two OH-stretching bands in β-FeOOH at 3475 and 3389 cm^{-1} can be a result of two slightly different OH sites [20], and this conclusion was supported with the structural refinement [21], indicating hydrogen bonds to be formed by oxygen atoms located on two crystallographically non-identical sites. In the case of H_2O molecules adsorbed onto β-FeOOH, the OH-stretching band corresponding to adsorbed H_2O is superimposed onto the OH-stretching bands of β-FeOOH. The IR bands at 843 and 698 cm^{-1} can be assigned to deformation vibrations of –OH groups, whereas the intensity of the shoulder at 642 cm^{-1} can be related to the interaction of the Fe–OH groups with Cl^- ions [22]. Weckler and Lutz [23] discussed two sets of vibrations at 847 and 820 cm^{-1}, as well as at

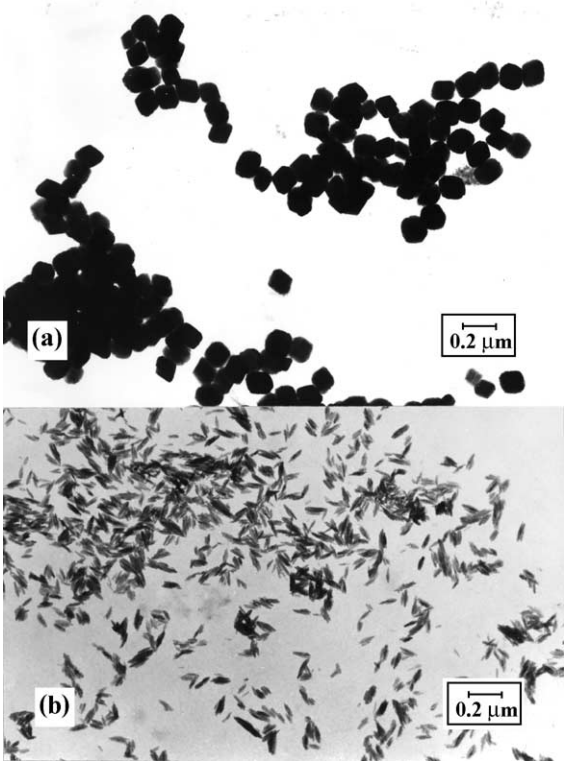

Fig. 4. TEM photographs of samples (a) S1 and (b) S2.

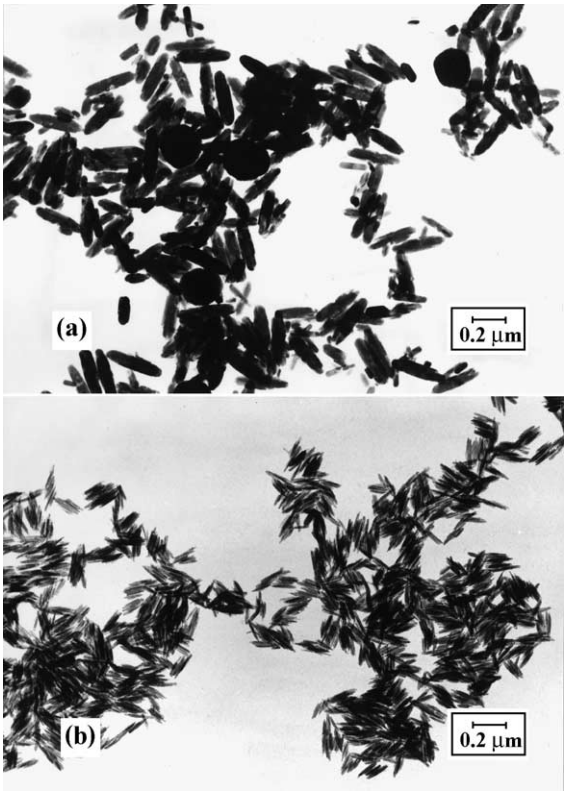

Fig. 5. TEM photographs of samples (a) S4 and (b) S6.

697 and 644 cm^{-1} in terms of two O—H···Cl hydrogen bonds present. Murad and Bishop [20] suggested that the weak shoulder at ~ 818 cm^{-1}, observed for the octahedral Fe—OH bonds in β-FeOOH, could be related to the nature of the OH-bending band near 820 cm^{-1} in smectites. β-FeOOH possesses a holandite-type structure [24,25] with the structural channels containing H_2O and a small amount of Cl^- ions.

The FT-IR spectrum of sample S10 shows β-FeOOH as the dominant phase and a small fraction of α-FeOOH, as concluded on the basis of the bands at 895 and 795 cm^{-1}. In this spectrum, the IR bands of adsorbed sulphates are also visible, similar as in the FT-IR spectrum of sample S2.

TEM showed a variety of particle shapes formed by forced hydrolysis of $FeCl_3$ solutions under physico-chemical conditions given in Table 1. Fig. 4a shows uniform α-Fe_2O_3 particles produced by forced hydrolysis of the 0.01 M $FeCl_3$ solution for 7 days (sample S1). With the addition of 0.005 M QHS to this precipitation system small particles were obtained (sample S2), composed of a few laterally aggregated α-FeOOH needles (Fig. 4b). Fig 5a shows a mixture of β-FeOOH and α-Fe_2O_3 particles produced by forced hydrolysis of the 0.02 M $FeCl_3$ solution for 7 days (sample S4). Cigar-shaped β-FeOOH particles showed irregular ends and surfaces due to their dissolution, whereas α-Fe_2O_3 particles were close to a spherical shape. The addition of 0.05 M HCl + 0.005 M QHS at the beginning of this precipitation process caused the formation of small α-FeOOH needles (sample S6), which also showed a tendency towards lateral aggregation (Fig. 5b). Fig. 6a shows β-FeOOH particles produced by forced hydrolysis of the 0.1 M $FeCl_3$ + 0.005 M HCl solution for 1 day (sample S11). Cigar-shaped and X-shaped β-FeOOH particles are visible, typical of β-FeOOH colloids. The addition of 0.005 M QHS to this precipitation system strongly changed the morphology of β-FeOOH particles (sample S12), as is visible in Fig.

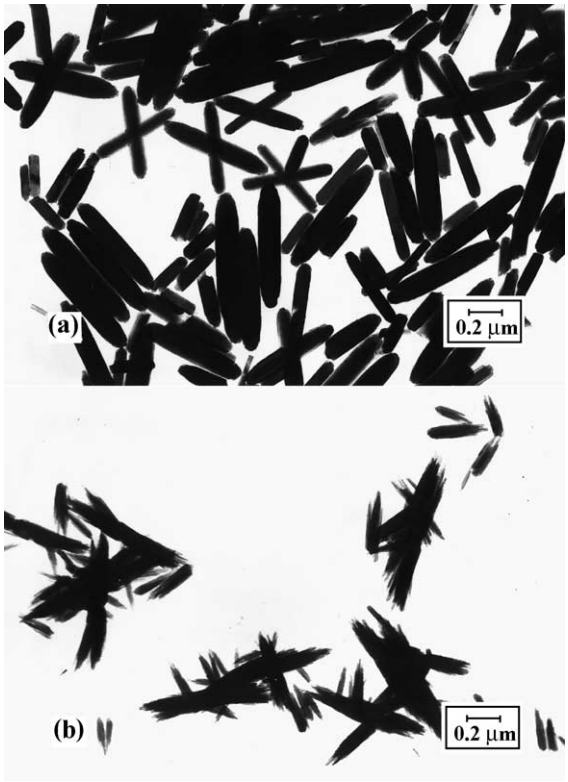

Fig. 6. TEM photographs of samples (a) S11 and (b) S12.

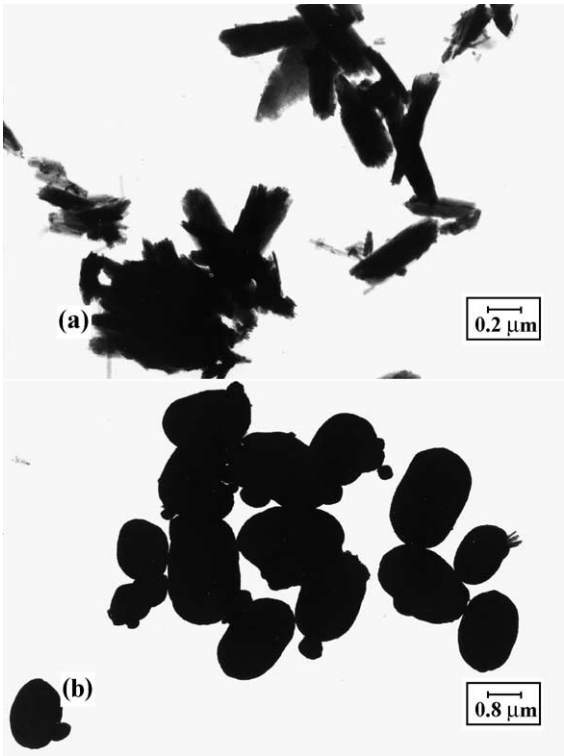

Fig. 7. TEM photographs of samples (a) S15 and (b) S16.

6b. This effect was observed for all β-FeOOH particles formed in the presence of QHS. The formation of the bundles of β-FeOOH needles could be ascribed to a possible complexing role of quinine at the very beginning of hydrolysis of Fe^{3+} ions and a specific adsorption of sulphates on the crystal planes along *c*-axis of β-FeOOH. Forced hydrolysis of the solution 0.1 M $FeCl_3$ + 0.05 M HCl + 0.005 M QHS (sample S15) yielded α-FeOOH particles after 7 days and the morphology of these particles (Fig. 7a) is different from that observed for α-FeOOH particles produced at lower $FeCl_3$ concentrations (samples S2 and S6). The particles of sample S15 are also composed of α-FeOOH needles; however, these secondary particles are much bigger. Finally, forced hydrolysis of the 0.1 M $FeCl_3$ + 0.1 M HCl solution yielded α-Fe_2O_3 particles (sample S16), as shown in Fig. 7b. It is well visible that these α-Fe_2O_3 particles are much bigger than those produced from the 0.01 M $FeCl_3$ solution over the same time of hydrolysis. In the presence of 0.005 M QHS there was no visible precipitate over the same time of hydrolysis (precipitation system S17).

The present work indicates that in the presence of 0.005 M QHS, the formation of goethite is favoured. The preferential adsorption of sulphate groups influenced the morphology of iron oxide particles, whereas the influence of quinine group at the very beginning of $FeCl_3$ hydrolysis via quinine–iron interactions cannot be excluded [26]. At high sulphate concentrations the formation of basic iron(III)-sulphates is favoured. It is generally assumed that this mechanism is directed by the $FeSO_4^+$ complex which strongly suppresses the polymerisation of Fe(III)-hydroxy complexes [27–30].

Acknowledgements

The authors wish to thank Prof. Nikola Ljubešić for his valuable help in the electron microscopic work.

References

[1] R.M. Cornell, U. Schwertmann, The Iron Oxides, Structure, Properties, Reactions, Occurrence and Uses, VCH Publ., D-69451 Weinheim, Germany, 1996.
[2] C.M. Flynn Jr., Chem. Rev. 84 (1984) 31.
[3] W. Schneider, B. Schwyn, The hydrolysis of iron in synthetic, biological, and aquatic media, in: W. Stumm (Ed.), Aquatic Surface Chemistry: Chemical Processes at the Particle–Water Interface, Wiley, 1987, p. 167.
[4] E. Matijević, J. Colloid Interface Sci. 58 (1977) 374.
[5] E. Matijević, P. Scheiner, J. Colloid Interface Sci. 63 (1978) 509.
[6] S. Musić, A. Vértes, G.W. Simmons, I. Czakó-Nagy, H. Leidheiser Jr., J. Colloid Interface Sci. 85 (1982) 256.
[7] M. Gotić, S. Popović, N. Ljubešić, S. Musić, J. Mater. Sci. 29 (1994) 2474.
[8] S. Musić, M. Gotić, N. Ljubešić, Mater. Lett. 25 (1995) 69.
[9] K. Kandori, A. Yasukawa, T. Ishikawa, J. Colloid Interface Sci. 180 (1996) 446.
[10] K. Kandori, Y. Nakamoto, A. Yasukawa, T. Ishikawa, J. Colloid Interface Sci. 202 (1998) 499.
[11] K. Kandori, A. Yasukawa, T. Ishikawa, Ind. Eng. Chem. Res. 39 (2000) 2635.
[12] M. Ozaki, S. Kratohvil, E. Matijević, J. Colloid Interface Sci. 102 (1984) 146.
[13] N.J. Reeves, S. Mann, J. Chem. Soc. Faraday Trans. 87 (1991) 3875.
[14] M.P. Morales, T. Gonzáles-Carreño, C.J. Serna, J. Mater. Res. 7 (1992) 2538.

[15] T. Sugimoto, A. Maramatsu, J. Colloid Interface Sci. 184 (1996) 626.
[16] M. Ocaña, M.P. Morales, C.J. Serna, J. Colloid Interface Sci. 212 (1999) 317.
[17] J.E. Iglesias, C.J. Serna, Miner. Petrogr. Acta 29A (1985) 363.
[18] C. Morterra, A. Chiorino, E. Borello, Mater. Chem. Phys. 10 (1984) 119.
[19] S. Musić, A. Šarić, S. Popović, K. Nomura, T. Sawada, Croat. Chem. Acta 73 (2000) 541.
[20] E. Murad, J.L. Bishop, Am. Mineral. 85 (2000) 716.
[21] J.E. Post, V.F. Buchwald, Am. Mineral. 76 (1991) 272.
[22] A. Šarić, S. Musić, K. Nomura, S. Popović, Mater. Sci. Eng., B 56 (1998) 43.
[23] B. Weckler, H.D. Lutz, Eur. J. Solid State Inorg. Chem. 35 (1998) 531.
[24] S.T. Galbraith, T. Baird, J.R. Fryer, An investigation of the dehydration of β-iron oxyhydroxide, Inst. Phys. Conf. Ser. No 52 C, 1980, pp. 291–294, Chap. 5.
[25] N.G. Holm, Origins of Life 15 (1985) 131.
[26] D.C. Warhurst, Biochem. Pharmacol. 30 (1981) 3323.
[27] E. Matijević, R.S. Sapieszko, J.B. Melville, J. Colloid Interface Sci. 50 (1975) 567.
[28] S. Musić, Z. Orehovec, S. Popović, I. Czakó-Nagy, J. Mater. Sci. 29 (1994) 1991.
[29] K. Parida, J. Das, J. Colloid Interface Sci. 178 (1996) 586.
[30] T. Sugimoto, Y. Wang, J. Colloid Interface Sci. 207 (1998) 137.